J|A|C|S
ARTICLES

Published on Web 04/05/2010

Decoding Circulating Nucleic Acids in Human Serum Using Microfluidic Single Molecule Spectroscopy

Kelvin J. Liu,[†] Malcolm V. Brock,[§] Ie-Ming Shih,[||] and Tza-Huei Wang*[,†,‡]

Biomedical Engineering Department, Mechanical Engineering Department, 3400 North Charles Street, Johns Hopkins University, Baltimore, Maryland 21218 and Divisions of Thoracic Department of Surgery, Departments of Pathology, Oncology, Gynecology and Obstetrics, Johns Hopkins Medical Institutions, Baltimore, Maryland 21231

Received January 14, 2010; E-mail: thwang@jhu.edu

Abstract: Circulating nucleic acid (CNA) has been the focus of recent research as a noninvasive source of biomarker candidates. Among these markers, DNA fragment size has shown promise for discerning the source of CNA molecules in cancer and prenatal diagnostics. We have developed a one-step assay for analyzing circulating DNA size and quantity directly in human serum. Microfluidic cylindrical illumination confocal spectroscopy and fluorescence burst size analysis are used to individually count and size fluorescently-labeled CNA molecules as they are driven through a microfluidic constriction. First, single molecule sizing was performed on λ Hind III digest DNA to obtain a size calibration curve. A linear relation between DNA length and burst size was seen from 564 bp to 27.5 kbp. Subsequently, the single molecule assay parameters were optimized. Finally, DNA sizing analysis was performed on serum samples from both early and late stage lung cancer patients. This assay was performed directly in patient serum using only a single reagent, a simple DNA intercalating dye, and without the need for DNA isolation or enzymatic amplification steps. This demonstrates that microfluidic single molecule spectroscopy can be a rapid, facile, and inexpensive alternative to the established PCR-based methods that have been used near exclusively for CNA analysis.

Introduction

Circulating and cell-free nucleic acid (CNA) consists of extracellular genetic material freely found in human body fluids. These information-rich molecules are a near ideal source of noninvasive biomarkers as they are readily released into the body from both pathologic and healthy cells. They are being extensively studied in a diverse array of human diseases such as cancer, fetal medicine, and diabetes.[1] In cancer, CNA can be used to noninvasively determine the status of remote tumors by decoding the contained genetic and epigenetic information, potentially bypassing the need for tissue biopsies. They have been demonstrated throughout cancer management in the assessment of tumor dynamics, therapeutic response, disease progression, and prognosis.[2−4] However, the clinical analysis of CNA biomarkers faces two key hurdles. First, CNA is present at low physiological concentrations, and second, the CNA of interest must be accurately discerned from a sea of obscuring background CNA.[5] To date, PCR-based methods have been used near exclusively for their analysis. While PCR is highly sensitive, it has intrinsic limitations such as amplification errors, varying amplification efficiencies, and reproducibility.[6] Thus, rapid and inexpensive alternatives to PCR can provide scientists with additional tools to more efficiently validate these markers.

Circulating DNA size has promising implications in cancer management[3,4,7] and fetal medicine.[8] The presence of long circulating DNA strands (i.e. increased DNA integrity) has been suggested to be indicative of neoplastic disease.[4,9] Accordingly, DNA integrity has been used as a general cancer marker in a wide variety of cancers.[3,4,7] In fetal medicine, circulating fetal DNA has been shown to be shorter than maternal DNA.[10] This

[†] Biomedical Engineering Department, Johns Hopkins University.
[‡] Mechanical Engineering Department, Johns Hopkins University.
[§] Divisions of Thoracic Department of Surgery, Johns Hopkins Medical Institutions.
[||] Departments of Pathology, Oncology, Gynecology and Obstetrics, Johns Hopkins Medical Institutions.

(1) Swarup, V.; Rajeswari, M. R. *FEBS Lett* **2007**, *581*, 795–9. Tong, Y. K.; Lo, Y. M. *Clin. Chim. Acta* **2006**, *363*, 187–96.
(2) Diehl, F.; Schmidt, K.; Choti, M. A.; Romans, K.; Goodman, S.; Li, M.; Thornton, K.; Agrawal, N.; Sokoll, L.; Szabo, S. A.; Kinzler, K. W.; Vogelstein, B.; Diaz, L. A., Jr. *Nat. Med.* **2008**, *14*, 985–90.
(3) Umetani, N.; Giuliano, A. E.; Hiramatsu, S. H.; Amersi, F.; Nakagawa, T.; Martino, S.; Hoon, D. S. *J. Clin. Oncol.* **2006**, *24*, 4270–6.
(4) Wang, B. G.; Huang, H. Y.; Chen, Y. C.; Bristow, R. E.; Kassauei, K.; Cheng, C. C.; Roden, R.; Sokoll, L. J.; Chan, D. W.; Shih Ie, M. *Cancer Res.* **2003**, *63*, 3966–8.
(5) Fleischhacker, M.; Schmidt, B. *Biochim. Biophys. Acta* **2007**, *1775*, 181–232.
(6) Diehl, F.; Diaz, L. A., Jr. *Curr. Opin. Oncol.* **2007**, *19*, 36–42.
(7) Chan, K. C.; Leung, S. F.; Yeung, S. W.; Chan, A. T.; Lo, Y. M. *Clin. Cancer Res.* **2008**, *14*, 4141–5. Umetani, N.; Kim, J.; Hiramatsu, S.; Reber, H. A.; Hines, O. J.; Bilchik, A. J.; Hoon, D. S. *Clin. Chem.* **2006**, *52*, 1062–9.
(8) Li, Y.; Di Naro, E.; Vitucci, A.; Zimmermann, B.; Holzgreve, W.; Hahn, S. *Jama* **2005**, *293*, 843–9. Lun, F. M.; Tsui, N. B.; Chan, K. C.; Leung, T. Y.; Lau, T. K.; Charoenkwan, P.; Chow, K. C.; Lo, W. Y.; Wanapirak, C.; Sanguansermsri, T.; Cantor, C. R.; Chiu, R. W.; Lo, Y. M. *Proc. Natl. Acad. Sci. U.S.A.* **2008**, *105*, 19920–5.
(9) Jahr, S.; Hentze, H.; Englisch, S.; Hardt, D.; Fackelmayer, F. O.; Hesch, R. D.; Knippers, R. *Cancer Res.* **2001**, *61*, 1659–65.
(10) Chan, K. C.; Zhang, J.; Hui, A. B.; Wong, N.; Lau, T. K.; Leung, T. N.; Lo, K. W.; Huang, D. W.; Lo, Y. M. *Clin. Chem.* **2004**, *50*, 88–92.

Scheme 1. Schematic Illustration of the One-Step, PCR-Free, Single Molecule CNA Sizing Assay

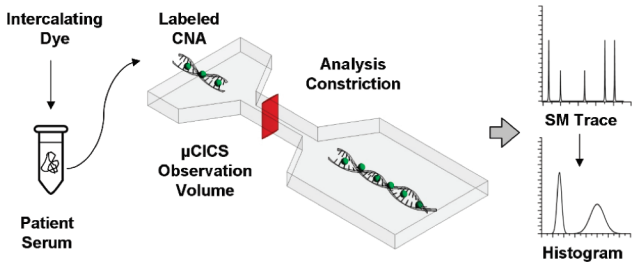

size difference has been used to enrich rare fetal DNA from a sea of maternal DNA for increased specificity in noninvasive prenatal diagnostics.[8] Thus, DNA size can be a key discriminating factor in identifying the source of CNA molecules. Previous studies have used nested qPCR to size DNA, a cumbersome approach that may be contributing to the variability in reported results.

We have previously shown that confocal spectroscopy (CS) can detect femtomolar to nanomolar levels of DNA,[11,12] a range that overlaps the physiological levels of CNA. Herein, we demonstrate the first PCR-free, single molecule assay for CNA analysis. Microfluidic cylindrical illumination confocal spectroscopy (μCICS) was used to size and quantify CNA fragments in human serum as illustrated in Scheme 1. μCICS uses a 1-D observation volume expansion and matched microfluidic constriction to achieve high detection uniformity, 100% mass detection efficiency, and higher throughput than conventional, diffraction-limited CS systems.[13] First, this platform was calibrated and optimized by sizing λ Hind III digest DNA. Then, the ability of the assay to analyze CNA size was validated by testing a small number of serum samples from stage I and stage IV lung cancer patients. This assay used only a single reagent, was performed directly in serum without the need for DNA isolation or separation, and consumed <10 pL of sample.

Experimental Section

***μ*CICS Platform.** An optical schematic and image are shown in Figure 1. The μCICS platform has two overlapping excitation and detection channels. 488/520 nm excitation/detection was used to monitor the tracer particle fluorescence while 633/670 nm excitation/detection was used to analyze the DNA fluorescence. Briefly, a 633 nm He−Ne laser (Melles Griot, Carlsbad, CA) and 488 nm Ar-ion laser (Melles Griot, Carlsbad, CA) were combined using a dichroic mirror, DM (z633RDC, Chroma Technology), and coupled into a polarization preserving single mode optical fiber, SM-Fiber (Melles Griot, Carlsbad, CA). The output from the fiber was collimated, expanded using a Keplerian beam expander, and focused in 1-D with an $f = 300$ mm cylindrical lens, CL (Thorlabs, Newton, NJ). A 1/2 waveplate, WP (Melles Griot, Carlsbad, CA), was used to align the laser polarization at a 57° angle with respect to the microchannel.[14] The laser excitation sheet was focused into the center of the analysis constriction on the microfluidic device with a 100×, 1.3 NA oil immersion microscope objective, OBJ (UPlanFl, Olympus, Center Valley, PA). The focused illumination volume, shown in Figure 1b, had $1/e^2$ radii of $x_0 = 18$, $y_0 = 0.5$, and $z_0 = 2.1$ μm where x_0, y_0, and z_0 align with the channel width,

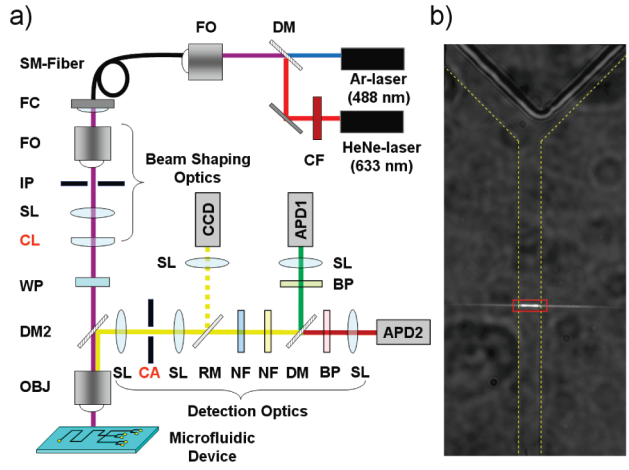

Figure 1. (a) Optical component diagram of μCICS platform. (b) CCD image of the μCICS illumination sheet focused into the microfluidic analysis constriction. The channel boundaries are demarcated by dashed yellow lines, while the projection of the confocal aperture into sample space is shown in red.

length, and height, respectively. 0.8 mW and 2.3 mW of blue and red laser power were used unless otherwise indicated. Excitation laser power was measured at the laser fiber output. The emitted fluorescence was then collected by the same objective, separated from the excitation light using a dichroic mirror, DM2 (z488/633rpc, Chroma Technology, Bellows Falls, VT), and filtered by a custom made, 600 μm × 150 μm ($w \times h$) rectangular confocal aperture, CA (National Aperture, Salem, NH). The confocal aperture limited light collection to the centermost 7 μm of the 36 μm wide illumination sheet where the illumination intensity was most uniform as depicted in Figure 1b. This created a 7 μm × 2 μm ($w \times h$) observation region that was slightly larger than the 5 μm × 0.5 μm ($w \times h$) analysis constriction to ensure 100% mass detection efficiency, simple alignment, and high detection uniformity. Holographic notch filters, NF (Kaiser Optical Systems, Ann Arbor, MI), were used to reduce the laser scattering background. A series of dichroic mirrors, DM, and band-pass filters, BP (Omega Optical, Brattleboro, VT), was then used to separate and select the desired fluorescence wavelengths before being detected with two APDs (SPCM-AQR13, Perkin-Elmer, Vaudreuil, Quebec, Canada). The output signal from the APDs was sent into a computer for analysis using software written in Labview (National Instruments, Austin, TX). A CCD camera was used to align the μCICS observation volume with the analysis constriction.

***μ*CICS Analysis.** PDMS microfluidic devices were fabricated with standard soft-lithography techniques. Each microfluidic device contained a large transport channel with a centrally located analysis constriction as shown in Scheme 1. The analysis constriction measured either 5 μm × 1.5 μm or 5 μm × 0.5 μm ($w \times h$). All experiments except for the laser power experiments were performed in the 0.5 μm deep channels. To reduce channel clogging, the device incorporated a filter array at the inlet to remove stray particles and cells. Samples were driven through the device using a nitrogen pressure source controlled by a series of precision gas regulators. Flow velocity and stability were monitored in situ using fluorescent tracer particles as described below. Piezoelectric stages were used to focus the μCICS laser into the center of the analysis constriction. Each single molecule trace consisted of 300 s of data collected with a 0.1 ms bin time.

Data Analysis. Software written in Labview (National Instruments, Austin, TX) was used to acquire and process the single molecule trace data. The data were processed in three stages. First, the raw traces were corrected to account for the APD nonlinearity. At this stage, smoothing algorithms such as Lee filters and moving average filters could also be applied, though these were not used. Second, a thresholding algorithm was applied to each single

(11) Zhang, C. Y.; Yeh, H. C.; Kuroki, M. T.; Wang, T. H. *Nat. Mater.* **2005**, *4*, 826–31.
(12) Wang, T. H.; Peng, Y.; Zhang, C.; Wong, P. K.; Ho, C. M. *J. Am. Chem. Soc.* **2005**, *127*, 5354–9.
(13) Liu, K. J.; Wang, T. H. *Biophys. J.* **2008**, *95*, 2964–75.
(14) Werner, J. H.; Larson, E. J.; Goodwin, P. M.; Ambrose, W. P.; Keller, R. A. *Appl. Opt.* **2000**, *39*, 2831–9.

molecule trace to identify fluorescent bursts. This threshold was a minimum of 3σ greater than the average background level to ensure high confidence burst identification. A burst was identified when the fluorescent intensity crossed the threshold value. The beginning and end of each burst were signified when the fluorescent intensity returned to the baseline value. The identified bursts were then analyzed for fluorescent burst parameters including burst height, burst size, and transit time and saved into an output file. Finally, the identified burst parameters were histogrammed, and the histograms were saved as a second output file. A screenshot of the software is included in Supporting Figure S-1. For the DNA sizing calibrations, a least-squares curve fit analysis was performed on the histograms using OriginPro 8 (Origin Lab Corp, Northamptom, MA).

Fluorescent Tracer Particle. 0.04 μm yellow-green Fluospheres (Invitrogen, Carlsbad, CA) were mixed into each sample and used to monitor sample flow velocity. The stock solution was first diluted 1000-fold in TE buffer. 2 μL of the diluted bead solution were then added to each sample immediately before μCICS analysis. For the clinical samples, the drive pressure was adjusted until an average particle transit time of 5 ms was achieved. This corresponded to an average flow velocity of 0.2 mm/s within the microchannel and ensured that the flow velocity remained constant across all experiments, chips, and samples. Typical drive pressures ranged from 0.01 to 4 psi depending on specific device geometry.

DNA Sizing Calibrations. λ Hind III digest DNA (New England Biolabs, Ipswich, MA) was used as a sample for assay development. To prepare the sample for analysis, the DNA was diluted and mixed with TOTO-3 dye (Invitrogen, Carlsbad, CA) at DNA and dye concentrations of 200 ng/mL and 0.1 μM, respectively. The mixture was allowed to incubate at room temperature in the dark for 1 h. The sample was then further diluted to a 1 pM individual fragment concentration and loaded into the microfluidic device for analysis. All dilutions were performed using TE buffer.

Control Samples. Three control samples were prepared. First, λ Hind III digest DNA was labeled with TOTO-3 as described above and mixed with 150-fold diluted serum to test the effect of the serum background on DNA sizing resolution. Second, 15 μL of 0.2 μM of TOTO-3 were mixed with 15 μL of 7.5% bovine serum albumin (Sigma, St. Louis, MO) to approximate a physiological concentration of blood protein. The sample was then mixed with TE buffer and 2 μL of diluted fluorescent beads to a total of 150-fold dilution for μCICS analysis. Third, serum was diluted 150-fold in TE buffer and mixed with fluorescent beads without TOTO-3 for μCICS analysis.

Clinical Sample Analysis. The serum samples were anonymously retrieved from Johns Hopkins Hospital and were approved by the local institutional review board. 20 μL of patient serum sample were mixed with 20 μL of 0.2 μM TOTO-3 dye. The samples were allowed to react for 1 h after which they were diluted a total of 150-fold in TE buffer. Fluorescent tracer particles were then added to the diluted sample, and the sample was loaded into the μCICS system for analysis. The flow velocity was adjusted to obtain a particle transit time of 5 ms. DNA sizing was performed after a stable flow velocity was obtained. λ Hind III digest DNA was analyzed identically to obtain a size calibration curve.

Results

First, fluorescent burst size analysis was performed on λ Hind III digest DNA to obtain a size calibration curve. As depicted in Scheme 1, the DNA was stoichiometrically labeled with TOTO-3 intercalating dye such that each DNA molecule incorporated a number of dye molecules that was directly proportionate to its length. The labeled sample was diluted, fluorescent tracer particles were added, and the sample was loaded into a microfluidic device. The μCICS observation volume was then focused into the center of the analysis constriction. As each DNA molecule traversed the observation volume, it was excited and emitted a burst of photons. This procession of fluorescent signals formed a single molecule trace. A thresholding algorithm was used to identify fluorescent bursts within the trace. These bursts were then analyzed for parameters such as burst size, burst width, and transit time.

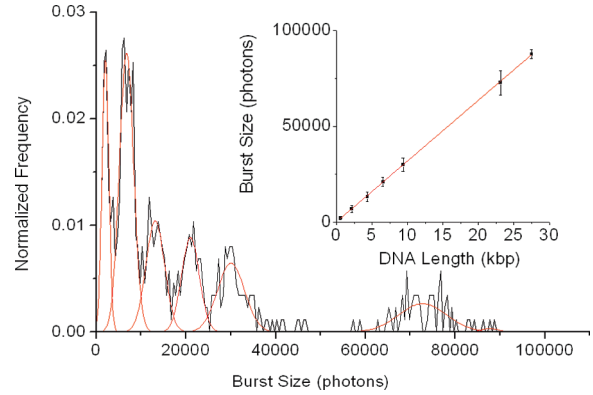

Figure 2. Fluorescent burst size analysis of λ Hind III digest DNA performed using μCICS. (Inset) The average burst size of each peak shows the expected linear correlation to DNA size ($R^2 = 0.9998$). Error bars represent the peak SDs.

The diffraction-limited laser excitation spot in standard CS precludes accurate DNA sizing due to the effects of molecular trajectory. In μCICS, the laser spot is expanded in 1-D to form a laser line that runs across the width of the microchannel using a cylindrical lens as shown in Figure 1b. A 600 μm $\times$ 150 μm rectangular confocal aperture, which mimics the shape of the desired observation volume, limits light collection to the center of the laser line where the illumination profile is most uniform to create a 7 μm $\times$ 2 μm ($w \times h$) observation region. A 5 μm $\times$ 0.5 μm ($w \times h$) microfluidic constriction is then used to transport molecules through the center of this observation region. Because the observation region fully encloses the analysis constriction, 100% mass detection efficiency (i.e., detection of all molecules flowing through the constriction) can be achieved and has been previously demonstrated for fluorescently labeled DNA as well as single fluorophores.[13] The 1-D observation volume expansion (i.e., from a point to a line) allowed uniform excitation and detection across the entire constriction cross section such that the fluorescent burst size was correlated only to DNA length and irrespective of molecular trajectory. Previous methods of controlling molecular trajectory have included nanochannel confinement, hydrodynamic focusing, and 3-D focal volume expansions.[15] The 1-D observation volume expansion enabled high uniformity while retaining high detection sensitivity.

A typical burst size histogram is shown in Figure 2. Each peak is a collection of fluorescent bursts that corresponds to a subpopulation of DNA within the Hind III digest. When the peaks were curve-fit with a series of Gaussian functions (red curves), a strong linear correlation was seen between average burst size (i.e. peak center position) and DNA length, demonstrating the ability to accurately size DNA from 564 bp to 27.5 kbp. The 2 kbp fragments were easily detected with a typical *S/N* ratio of ~80 and measurement coefficient of variation (CV) of ~25 %. The measurement CV prevented the 2027 bp and

(15) Chou, H. P.; Spence, C.; Scherer, A.; Quake, S. *Proc. Natl. Acad. Sci. U.S.A.* **1999**, *96*, 11–3. Foquet, M.; Korlach, J.; Zipfel, W.; Webb, W. W.; Craighead, H. G. *Anal Chem* **2002**, *74*, 1415–22. Habbersett, R. C.; Jett, J. H. *Cytometry A* **2004**, *60*, 125–34.

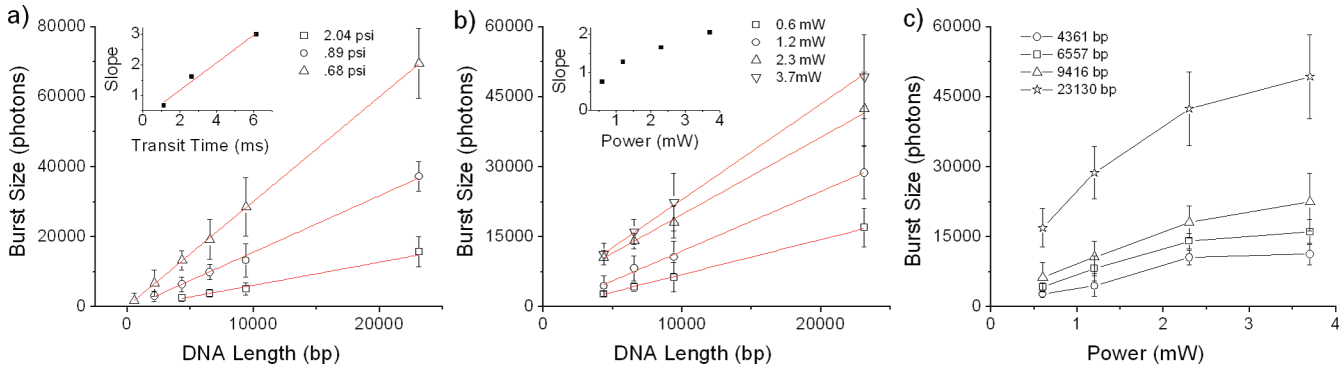

Figure 3. Laser power and flow velocity effects on μCICS fluorescent burst sizing of λ Hind III digest DNA. Each linear fit (red line) was taken from a burst size histogram consisting of at least 1000 peaks. Error bars represent peak fit SDs.

2322 bp peaks from being individually resolved and the 125 bp peak from being resolved from background. As expected, the measurement CV decreased with increasing DNA length due to factors such as Poisson variability in the photoemission and -detection processes and staining variability. The 23 kbp peak typically displayed a CV of 5−10 %. Detailed fit parameters are included in Supporting Table 1.

While the burst size can be used to determine DNA length, the burst rate can be used to determine relative abundance. Given the flow velocity, channel dimensions, and DNA concentration, ~520 molecules would be expected during each 300 s measurement whereas 590 molecules were actually detected, demonstrating 100% mass detection efficiency. The overestimation can be accounted for by small errors in the channel dimensions, measured flow velocity, observation volume size, and sample preparation. Supporting Table 1 also shows the relative detection frequency of each fragment population. Each population was properly enumerated at equal molar fractions with the composite 2.1 kbp peak having double the abundance (~30 %) of the other peaks (~15 %). A small number of 27.5 kbp fragments, which resulted from annealing of the 4.4 and 23.1 kbp fragments, was detected despite attempts to separate them by incubation at 65 °C.

To obtain accurate sizing data, measurement variables including flow rate, laser power, and constriction size were precisely controlled. In our experience when using low flow rates and elastomeric devices, flow driven by constant pressure sources displayed increased stability and lower settling time between adjustments than flow driven by constant flow rate sources such as syringe pumps. Thus, nitrogen pressure, controlled by a series of precision regulators, was used to drive flow. Because the sample flow rate and stability have such a large impact on sizing performance, fluorescent tracer particles were used to monitor the in situ flow velocity. Fluorescent tracer particles were used to measure molecular transit time as a function of drive pressure. The transit time was then used to calculate flow velocity. The flow velocity exhibited the expected linear relation to pressure demonstrating that the in situ velocity can be accurately monitored using the fluorescent tracer particles and that pressure can be used to accurately control flow velocity (Supporting Figure S-2). Therefore, fluorescent tracer particles were used to monitor and calibrate the in situ flow velocity in all subsequent DNA sizing measurements.

Generally speaking, slower flow rates led to higher precision single molecule measurements. As shown in Figure 3a, DNA sizing histograms were acquired at three different drive pressures to test the effect of flow velocity. As the flow velocity decreased, smaller DNA fragments were discerned from the background due to an increase in signal-to-noise ratio and decrease in measurement CV, thus demonstrating the need for flow velocity optimization in single molecule assays. The correlation between DNA length and fluorescent burst size became steeper at lower flow rates enabling higher precision measurements (Figure 3a inset). The flow velocity was set to long molecular transit times (~5 ms) to maximize signal intensity and minimize Poisson variability while remaining faster than molecular diffusion times (~25−250 ms).

To test the effects of laser excitation power, DNA sizing histograms were taken while the input laser power was changed from 0.6 to 3.7 mW. As seen in Figure 3b, the dependency of burst size on DNA size became steeper as the laser power increased. The steeper slope and lower measurement CV at higher laser powers resulted in higher DNA sizing resolution. This can be further seen by examining the 23.1 kb fragment in detail (Supporting Figure S-3). The average burst size increased with laser power while the measurement CV decreased. At 0.6 mW of power, the measurement CV substantially rose due to increased Poisson variability and a lower *S/N* ratio. Interestingly, when the fitted slopes of Figure 3b were plotted against laser power, the increase was not linear and showed saturation effects. This is further evident in Figure 3c where the burst size of each fragment is shown as a function of laser power. Because the sample contained individual populations of DNA molecules of disparate brightness but same color, it was seen that each population optically saturated at a different laser power. Longer DNA fragments containing more individual TOTO-3 dye molecules saturated at higher laser powers than shorter DNA with less dye. Though the mechanism is unclear, this effect cannot be accounted for by singlet state saturation. Thus, the laser power could only be optimally set for a single fragment population.

Finally, the effect of microfluidic analysis constriction size was tested. It has been previously shown that single fluorophore sensitivity and 100% mass detection efficiency can be achieved by coupling a 7 μm × 2 μm ($w \times h$) observation volume with a 5 μm × 2 μm ($w \times h$) microchannel.[13] Herein, DNA sizing histograms were taken using 5 μm × 0.5 μm or 5 μm × 1.5 μm ($w \times h$) analysis constrictions. Table 1 depicts measurement CVs for each DNA fragment population. The 1.5 μm deep constriction gave higher measurement CVs but allowed higher sample throughput, decreased the likelihood for clogging, and lowered drive pressures. The 0.5 μm constrictions gave lower measurement CVs but had more issues with flow stability. For

Table 1. DNA Sizing Measurement CVs for 0.5 μm and 1.5 μm Deep Analysis Constrictions in Buffer and Serum Backgrounds

DNA Fragment Size (kb)	Burst Size CV (%)		
	0.5 μm	1.5 μm	0.5 μm + serum
2.0 + 2.3	28	41	27
4.4	11	16	16
6.6	16	12	20
9.4	15	19	25
23.1	7	19	10

the subsequent clinical samples, 0.5 μm deep constrictions were used to obtain higher DNA sizing resolution.

Once the assay parameters were optimized, we tested whether the μCICS assay could be used to analyze CNA directly in serum without DNA isolation or PCR amplification. TOTO-3 was used because it fluoresces in the deep red (660 nm), far from most cellular autofluorescence. The high specificity and high fluorescent enhancement enabled separation-free analysis. The elimination of DNA isolation and purification reduced the potential bias introduced by these steps and streamlined analysis. TOTO-3 is also cell membrane impermeant, ensuring that only cell-free nucleic acids were labeled.

A one-step assay for analyzing CNA size was developed. Serum samples were mixed with TOTO-3 and incubated for 1 h. The labeled samples were then diluted, mixed with fluorescent tracer particles, and loaded into a microfluidic device. Figure 4a shows 10 s of representative single molecule trace data for a stage I cancer patient. Single molecule bursts arising from TOTO-3 labeled CNA molecules can clearly be seen above the background. A threshold of 40 photons, shown as a red dotted line, was used to identify fluorescent bursts. Control samples were tested to ensure that these bursts arose from CNA rather than nonspecific adsorption of TOTO-3 or sample autofluorescence. Few fluorescent bursts were seen when a physiological concentration of BSA (~7.5%), fluorescent tracer particles, and TOTO-3 were mixed and tested (Figure 4b), demonstrating that nonspecific adsorption of TOTO-3 to blood proteins and particles was negligible. In addition, there was also very little sample autofluorescence as can be seen in Figure 4c when the serum and particles were tested together under 633 nm excitation without TOTO-3. These results, along with the

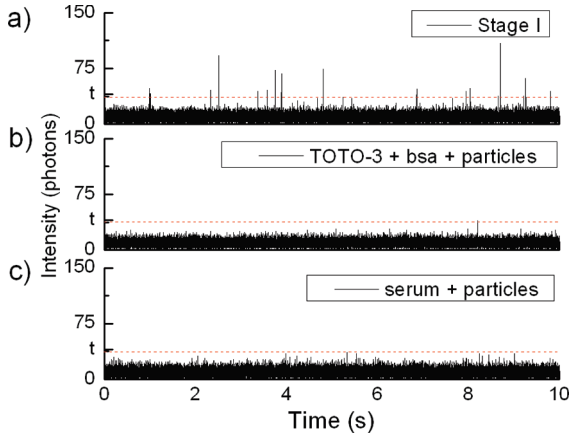

Figure 4. 10 s of representative μCICS single molecule trace data are depicted. (a) Stage I lung cancer patient serum sample; (b) TOTO-3, 7.5% BSA solution, and 0.04 μm fluorescent tracer particles; and (c) serum and 0.04 μm fluorescent tracer particles. The threshold (t = 40 photons) used to distinguish fluorescent bursts is indicated by a red dotted line.

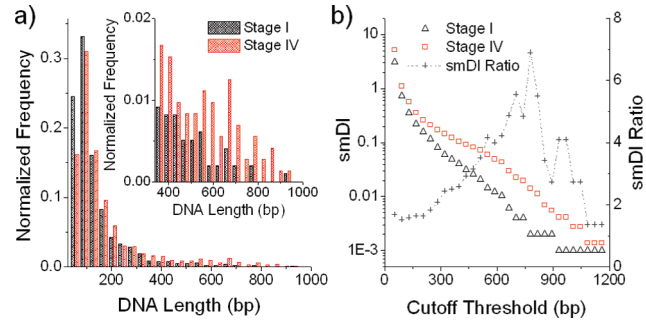

Figure 5. (a) Representative DNA sizing histograms of serum samples taken from stage I and stage IV lung cancer patients. (Inset) Close-up view of the 320−1000 bp region. (b) Single molecule DNA integrity (smDI) was calculated as a function of the cutoff threshold. The ratio of the smDI values for the two patients is also plotted.

high specificity of the TOTO-3 dye, suggest that the fluorescent signal can be attributed to CNA molecules only. A final control was performed to test whether the serum background would affect the DNA sizing resolution. λ Hind III digest DNA was prepared and analyzed identically as before but mixed with 150-fold diluted serum. This was the same dilution factor used for the subsequent clinical samples. Measurement CVs were only slightly decreased in serum as seen in Table 1. This was expected since the serum background in the deep red spectrum was very low, and the high sensitivity of μCICS allowed a high level of dilution.

The fluorescent bursts detected in the clinical samples were accumulated to form histograms. Figure 5a shows representative DNA sizing histograms for a stage I and a stage IV lung cancer patient. Qualitatively, it can be seen that the stage IV patient has a greater proportion of larger CNA fragments. Below 320 bp, the two curves appear similar. However, from 320 to 1000 bp, the stage IV sample consistently contains more fragments than the stage I sample (Figure 5a inset). Because nested qPCR is typically used, DNA integrity (DI), a quantitative marker of DNA fragmentation, is usually calculated as the ratio of long DNA fragments to short DNA fragments within the same gene or amplification locus (e.g., abundance of 400 bp vs 200 bp fragment of the β-actin gene).[3,4,7] On the other hand, since the single molecule assay was not limited to specific fragment sizes, we defined single molecule DNA integrity (smDI) as the cumulative number of long DNA bursts/short DNA bursts where the distinction between long and short is defined by a cutoff threshold. Direct digital counting eliminates the need for tedious calibration curves. Accordingly, Figure 5b shows smDI values calculated from the previous histograms as a function of the DNA cutoff threshold. The smDI values for the stage IV patient are consistently higher than that of the stage I patient. The optimal cutoff threshold can be set by selecting the point at which the greatest clinical differentiation occurs. The greatest distinguishing power occurred at a threshold of ~800 bp where the stage IV patient had an smDI value nearly 7-fold that of the stage I patient. The applied threshold can have a significant impact on the sensitivity and specificity of the marker and should be empirically set using a large sample size. Average smDI values for the patients tested in this preliminary study are presented in Supporting Table 2. While these results are too limited to draw any clinical conclusions from, they demonstrate that μCICS can be used as a facile alternative to PCR for quantifying CNA markers such DNA integrity. However, a

larger study will be necessary to determine the clinical sensitivity and specificity of the smDI marker in characterizing cancer progression.

In comparison, nested qPCR can only concurrently probe a limited number of DNA loci and sizes. The limited number of sampled loci may not be representative of the larger circulating population as a whole and lead to high variability while the limited DNA sizing resolution may hinder the accuracy of the DI marker. This can be particularly true in PCR reactions where only a few genome equivalents of DNA are tested. μCICS can directly reveal the entire spectrum of CNA fragments, without sampling bias or ensemble averaging, eliminating potentially significant sources of error.

Currently, molecular transit time variation arising from the Poiseuille flow profile is likely a significant contributor to the measurement CV. One potential way to reduce the CV, if necessary, is to use electrokinetic forces, including electroosmosis and electrophoresis, rather than pressure to drive flow. Electrokinetic drive results in plug−flow profiles that can significantly reduce transit time variations. Additionally, intercalating dyes with higher fluorescent enhancements and binding affinities can be explored to increase sensitivity and decrease the CV.

Whereas in these experiments a simple intercalating dye was used to detect and size CNA molecules, other types of fluorescent probes can be used to identify gene specific alterations or epigenetic changes that are indicative of disease. μCICS can be combined with fluorescent probes based on coincidence, FRET, and quenching to analyze other CNA markers such as SNPs, mutations, and methylation.[11,16,17] Alternatively, this sizing assay can be used in combination with other assays to increase specificity. For example, CNA sizing analysis can be used to first identify cancer or fetal CNA which can be subsequently isolated for further analysis.

Conclusion

We have detailed the development of a rapid and facile assay for CNA analysis based on μCICS, a microfluidic single molecule spectroscopy technique. We initially surmised that the overlap in dynamic range between single molecule sensing and physiological CNA levels would enable direct analysis of CNA markers without PCR amplification. We set out to show that, with proper assay design and probe selection, single molecule assays can be used to accurately analyze CNA even in complex biological backgrounds. To accomplish this, we chose DNA integrity as a model of a promising marker where the lack of alternatives to PCR-based methods may be limiting its application. Thus, in this initial proof of feasibility, we demonstrated that μCICS can be used to quantitatively analyze DNA integrity in human serum. Subsequently, a more exhaustive follow-up study is being performed to evaluate the accuracy of the smDI marker in the assessment of tumor dynamics. However, PCR and single molecule methods need not be mutually exclusive. We have previously combined CS and PCR to achieve ultrasensitive detection of methylation in cell-free DNA.[16] It is hoped that, with this demonstration, single molecule methods will be further explored to speed the clinical translation and adoption of new CNA biomarkers.

Acknowledgment. Financial support was provided by the NIH (Grants R21-CA120742-01 and U54-AI057168-06) and NSF (Grants 0546012, 0730503, and 0725528).

Supporting Information Available: Platform details, assay optimization data, and clinical testing results. This material is available free of charge via the Internet at http://pubs.acs.org.

JA100342Q

(16) Bailey, V. J.; Easwaran, H.; Zhang, Y.; Griffiths, E.; Belinsky, S. A.; Herman, J. G.; Baylin, S. B.; Carraway, H. E.; Wang, T. H. *Genome Res.* **2009**, *19*, 1455–61.

(17) Yeh, H. C.; Ho, Y. P.; Shih Ie, M.; Wang, T. H. *Nucleic Acids Res.* **2006**, *34*, e35.